Desalination and Water Treatment
www.deswater.com
doi: 10.5004/dwt.2021.26918

220 (2021) 159–167
April

Removal of nickel from the actual electrolytic wastewater by bentonite supported nanoscale zero valent iron

Bo Zhang, Bohong Zhu*, Xiong Wang, Songbai You, Bo Wang

School of Metallurgical and Material Engineering, Hunan University of Technology, Taishan Road 88, Zhuzhou 412007, Hunan, China, emails: bohongzhu@hut.edu.cn (B. Zhu), 181798320@qq.com (B. Zhang), 1658712931@qq.com (X. Wang), 3552419619@qq.com (S. You), 878440334@qq.com (B. Wang)

Received 3 June 2020; Accepted 1 December 2020

ABSTRACT

A large number of wastewater is produced in the process of electroplating industry, and pose serious threats to humanity. Nanoscale zero valent iron (nZVI) has a desirable reductive adsorption capacity for treatment of the electroplating wastewater, but limited by its agglomeration and oxidation. In this study, the composite material nZVI@B was prepared using the emulsion of nZVI and sodium bentonite, and characterized by scanning electron microscopy, X-ray diffraction, and X-ray photoelectron spectroscopy. The aggregation and oxidation phenomena of nZVI particles were decreased with the successfully supported on bentonite. The decontamination abilities of nZVI@B were tested by removal of nickel (Ni) from the electroplating wastewater. The results showed that the nZVI@B has a 99.96% removal efficiency at 120 min, which is greatly better than those of nZVI and bentonite. The reactivity of the nZVI can be effectively improved by dispersed in the interlayer of Bentonite and reduced to contact with water. The lower solution pH value, initial concentration, and higher dosage had positive effects on Ni removal. But the effect of temperature on final removal efficiency was not remarkable. Furthermore, the tailings obtained though the batch experiments were detected by energy-dispersive X-ray spectroscopy, the content of Ni is in the range from 25% to 40%, which can reduce the total amount of tailing slag treatment and the difficulty of recycling.

Keywords: Sodium bentonite; Removal of nickel; Electroplating wastewater; Nanoscale zero valent iron; Reduction

1. Introduction

Nickel is widely used in electroplating industry because of its hardness, corrosion resistance, and weldability [1–3]. However, a large number of heavy metal wastewater will inevitably be produced in the process of electroplating industry [4,5]. Nickel is a kind of heavy metal with carcinogenic characteristics [6]. It accumulates in human body and affects activity of biological enzymes [1]. Therefore, the treatment and discharge of electroplating wastewater have become an urgent problem.

Chemical precipitation method and membrane filtration method are the most commonly used to treat the electroplating wastewater in recent studies [7–10]. However, in the process of chemical precipitation, the pH value of wastewater needs to be adjusted for several times, resulting in a large number of generated neutralizing slag [7]. Moreover, to meet the discharge standard of China (the nickel content of emissions is not more than 0.5 mg/L, no. GB21900-2008) [11], a large number of flocculants and heavy metal capture agents are needed to be added, resulting in a series of problems, such as a high cost of chemicals and difficult treatment of tailings [7,8]. Membrane filtration method is used membrane to block specific elements and purify water [9,10]. With the improvement of membrane materials, this method has achieved good results in

* Corresponding author.

wastewater treatment. Yet, due to the membrane material is easy to be polluted during the treatment process as well as the high cost of membrane components, this technology still has room for improvement [10]. Moreover, the produced tailings belong to hazardous waste in China, which must be treated by the chemical precipitation method or membrane filtration method [12–14]. The cost of treatment tailings accounts for a large part of the total production cost.

As an advantageous water treatment material, nanoscale zero valent iron (nZVI) has been developed rapidly in recent 20 y [15–18]. An amount of research has been done on the remediation of organic and inorganic pollution in wastewater and contaminated soil, because of its simple operability and environmental friendliness [15,16]. However, there are still some technical problems should be solved in the use of the nZVI. First, Na_2BH_4 or K_2BH_4 is the main raw material for the preparation of nZVI, which leads to high production cost and difficulty in large-scale production [16–18]. Second, the nZVI particles are prone to agglomerate, resulting in the reduced reactive activity [17]. To overcome agglomeration shortcoming, many porous materials, such as active carbon [19,20], montmorillonite (MMT) [21], cryogels [22], vermiculite [23], and poly sodium acrylate [24], have been tested as the support to inhibit the aggregation of nZVI particles. Xie et al. [25] successfully supported nZVI on the reduced graphene oxide (rGO), which significantly reduced the aggregation of nZVI, and the removal effect of nZVI-rGO on trichloroethene was much higher than that of free NZVI.

Bentonite is a non-metallic mineral having the crystal structure of 2:1 layered silicate, which is composed of two silica tetrahedrons and one alumina octahedron [26]. Because of the existence of cations (such as Cu, Mg, Na, K, etc.) in the structure of bentonite soil layer, the interaction between these cations and crystal cells is very unstable, which makes bentonite have the excellent ion exchange capacity and can be used in wastewater treatment [27–29]. Yang et al. [29] prepared the composite hydrogel bead based on magnetic bentonite, chitosan and sodium alginate, and used it for adsorbing copper ions in wastewater. The results showed that the maximum adsorption capacity was 56.79 mg/g. Wang et al. [30] found that the adsorption capability of bentonite for U(VI) is obviously improved at low pH.

In recent years, several researches have investigated the bentonite-nZVI (nZVI@B) for treating the wastewater. Shi et al. [31] successfully synthesized nZVI@B by the sodium borohydride reduction method, and tested by aqueous Cr(VI) removal. The result showed that bentonite decreases the aggregation of nZVI particles. Li et al. [32] simulated the treatment of Cr(VI) in groundwater with nZVI@B, and found that the efficiency of the treatment of Cr(VI) by nZVI@B was much higher than that by free nZVI. The reduction process was in accordance with the pseudo first-order kinetic model, and the apparent rate constant K decreased with the decrease of the initial concentration of nZVI@B. However, it is rarely reported on the application of nZVI@B in the treatment of nickel from the actual electrolytic wastewater, and the removal mechanism and treatment kinetics of nickel wastewater treatment has not been clarified.

In this study, the emulsion of nZVI prepared by electrodeposition method was used as raw material, and supported on sodium bentonite to get composite material nZVI@B. The composite material and experimental products were characterized by X-ray diffraction (XRD), scanning electron microscopy (SEM), X-ray photoelectron spectroscopy (XPS), inductively coupled plasma-optical emission spectroscopy (ICP-OES), and energy-dispersive X-ray spectroscopy (EDX). The comprehensive mechanism for removal of Ni from wastewater by bentonite-supported nZVI in wastewater was proposed, and the influence factors were analyzed.

2. Materials and methods

2.1. Materials and chemicals

The nZVI emulsion was obtained by the impulse electro-deposition method, and the detailed preparation process can be found in our previous studies [33]. The size of nZVI particles was mainly 30–60 nm, and the total Fe concentration in the emulsion was 30 g/L. The sodium bentonite was supplied by Heng-Guang Mineral Products Co., Ltd., Hebei, China, with the particle size of 20 μm, density of 1.6 g/cm^3, and expansion ratio of 12.3. Other reagents, such as absolute ethanol (>98%), HCl (AR), and NaOH (AR), were purchased from Beihua Chemical Co., Ltd., Beijing, China. The deionized water was used throughout the experiments.

2.2. Synthesis of nZVI@B

The composite material was synthesized in a 500 mL conical flask, with 200 mL of nZVI emulsion and 100 mL of deionized water. The blended solutions were mixed under the sonication (Transsonic TI-H) for 30 min, and then 5 g of sodium bentonite was added. The supporting process was carried out using the mechanical mixer (IKA, Microstar 15) at 240 rpm for 30 min. During the mixing process, the space between the bottleneck, and the stirring rod was covered by the sealing film to avoid massive oxidation of materials. Finally, the mixed solution was filtered by vacuum filter (Sciencetool, FS3310), and the composite was washed for three times by anhydrous ethanol and dried in vacuum. 1 g of nZVI@B was dissolved by 5 mL HNO_3 (10 mol/L) and the concentration of Fe ions in acid solution were analyzed by ICP-OES. The total Fe content in the nZVI@B was calculated to be 17.46%.

2.3. Characterization

The micro morphology and mapping scan analysis of the sample were analyzed by scanning electron microscopy with energy dispersive spectrometer (SEM-EDX, SU8010, Tokyo, Japan). Before the SEM-EDX analysis, the sample was diluted and dispersed in absolute ethanol under ultrasonic for 15 min, then a few drops were deposited on the carbon-covered conductive tape and dried quickly by aurilave. The crystal structure and composition phase of samples were investigated by X-ray diffractometer (XRD, Ultima IV, Tokyo, Japan) scanned from 5° to 90° for 2θ with rate of 5°/min. The surface characteristics of nZVI@B were determined by XPS (Thermo ESCALAB 250XI; Massachusetts, USA). The concentration of metal ions in solution and tailings were detected by inductively coupled plasma

spectrometer (ICP-OES; PerkinElmer 8300, Massachusetts, USA) and energy dispersive X-ray spectrometer (EDX, EDX-720, Kyoto, Japan), respectively.

2.4. Adsorptive and reductive performances

The wastewater used in batch experiments was taken from an electroplating factory in Jingzhou (Hubei Province, China), with Ni content of 198.2 mg/L and pH value of 4.7. The total amount of other metal ions (Zn, Cu, and Cr) was less than 1.0 mg/L, so the influence of other metal ions for the experiments was ignored. The deionized water was used to dilute the wastewater to different concentrations (10, 40, 70, and 100 mg/L) for standby.

The batch experiments were carried out by adding the 200 mL diluted wastewater and the weighed material (Bentonite, nZVI, and nZVI@B) in a 500 mL conical flask, respectively. The conical flask was shocked on a thermomixer comfort (Jin-kong, ZW-A, China) at 240 rpm, and 5 mL of solution was taken out at 5, 10, 20, 30, 60, 90, and 120 min, respectively. After the batch experiment, the solution was filtered, and the obtained tailings were dried in vacuum. The initial pH value of wastewater (3.0, 7.0, and 10.0) was modified by adding 0.01 mol/L HCl or NaOH. The reaction temperatures (20°C, 40°C, and 60°C) were controlled by constant temperature water bath (Larksci, LWB-4, China). The removal efficiency and equilibrium removal capacity of Ni were calculated according to the Eqs. (1) and (2) [22]:

$$\eta(\%) = \frac{\left(C_0 - C_t\right)}{C_0} \times 100 \tag{1}$$

$$q_e = \frac{\left[\left(C_0 - C_e\right) \times V\right]}{w} \tag{2}$$

where η (%) is the removal efficiency of Ni from wastewater. C_0 (mg/L), C_t (mg/L), and C_e (mg/L) represent the concentrations of Ni in wastewater at initial time, t time, and equilibrium time, respectively. q_e (mg/g) is the removal capacity of Ni at equilibrium, V (L) is the solution volume, and w (g) is the dry weight of metals.

The pseudo-first-order (PFO, Eq. (3)) and pseudo-second-order (PSO, Eq. (4)) [33] equations were employed to quantitatively describe the adsorption kinetics of Ni from wastewater as following:

$$\ln\left(q_e - q_t\right) - \ln q_e = -k_1 t \tag{3}$$

$$\frac{t}{q_t} - \frac{t}{q_e} = \frac{1}{k_2 q_e^2} \tag{4}$$

where q_t (mg/g) is the removal capacity of Ni at t time; k_1 (min^{-1}) and k_2 (g/(mg min)) represent the equilibrium rate constants of PFO and PSO model, respectively.

3. Results and discussions

3.1. Characterization

As shown in Figs. 1a and b, the nZVI particles prepared by impulse electro-deposition method can be dispersed in absolute ethanol under the ultrasonic condition. Bentonite can be well-dispersed into starch gel in water, which provides favorable condition for successful immobilization of nZVI particles. After being deposited and dried on the carbon-covered conductive tape, bentonite piles up together, resulting in the layered structure, as shown in Figs. 1c and d.

The XRD patterns of nZVI, bentonite, nZVI@B before and after reaction are shown in Fig. 2. The pattern of nZVI

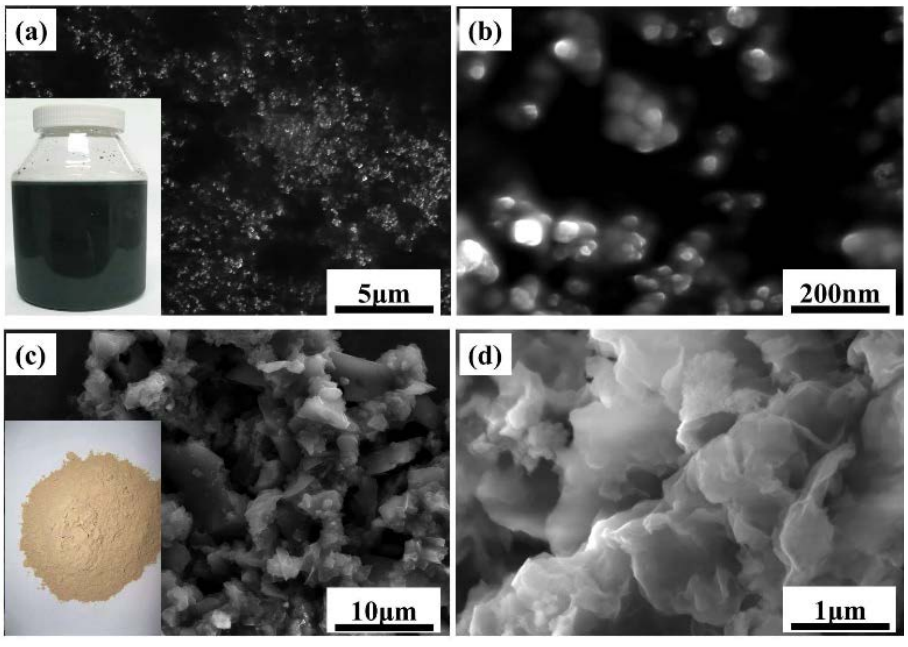

Fig. 1. SEM micrographs of nZVI and sodium bentonite, (a) and (b) nZVI, (c) and (d) bentonite.

shows three diffraction peaks at 2θ value of 18.1°, 22.2°, and 26.6° corresponding to (105), (223), and (116) Fe_2O_3, and a diffraction peak at 38.7° corresponding to (111) of Fe^0, respectively [31]. The diffraction peak of nZVI is weak, indicating the nZVI particles prepared by impulse electrodeposition method is extremely small with the limited crystallization degree [32]. The main components of bentonite are SiO_2 and aluminosilicate (Al_2SiO_5 and $NaAlSi_3O_8$) as shown in the pattern (b). The pattern (c) shows two additional peak at 2θ value of 36.5° and 61.9° corresponding to FeO, and it declares the successful supported of nZVI. There is no peak of Fe^0 on the XRD patterns of nZVI@B before and after reaction, which may be due to the poor crystallinity of Fe^0 or the formation of oxide film on the surface during the reaction. The peak at 2θ value of 21.0°, 34.8°, and 39.5° corresponding to the taenite ([Fe,Ni]) after reaction with wastewater for 2 h as shown in the pattern (d), indicating that Ni can be adsorbed on the surface of nZVI@B.

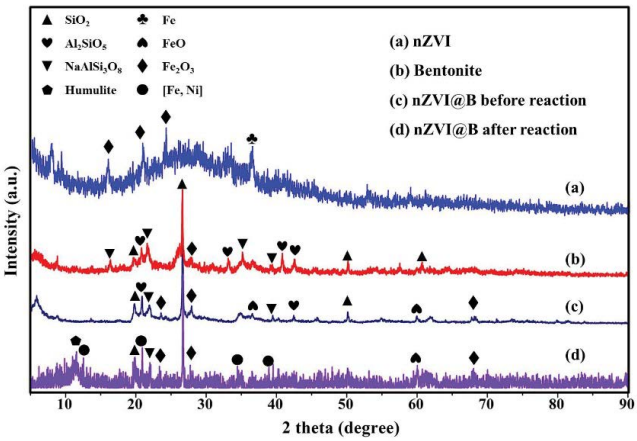

Fig. 2. X-ray diffraction (XRD) patterns of nZVI, bentonite, nZVI@B before and after reaction.

The nZVI@B compounded by mechanical stirring method was dried and broken, and its micrographs and mapping scan are shown in Fig. 3. For the fresh nZVI@B, a large number of nZVI particles adhere to the interlayer of bentonite individually as stacked layers, as clearly shown in Figs. 3a and d. Moreover, the mapping scan shows the distributions of Fe, Na, Si, and Al on the interlayer of nZVI@B, as shown in Figs. 3b, c, e, and f. The distributions of Fe and Na are remarkably synchronous, which confirms that the supported process of nZVI is related to the cations in the structure of bentonite soil layer. Therefore, the layered structure of bentonite effectively prevents the aggregation of the nZVI particles, which is beneficial to the exposure of active sites, so as to promote the reactivity of nZVI.

The XPS spectra of nZVI@B after reaction was analyzed to study the transformation process of Fe and Ni in the reaction process, as shown in Fig. 4. In Fig. 4a, the peaks of Fe 2p and Ni 2p appears at the range of 711.95 and 856.65 eV, respectively [34]. The high-resolution XPS spectra of Fe 2p orbit is displayed, and can be divided into four peaks, as shown in Fig. 3b. The Fe^{3+} peak appears at 711.6 and 725.3 eV, and the Fe^{2+} peak appears at 710.0 and 722.7 eV, respectively [32]. However, the peak of Fe^0 in XPS spectrum has not been detected, which is due to the rapid formation of iron oxide on the surface of nZVI particles, and the limitations of the detection depth for XPS technology [31]. The high-resolution XPS spectra of Ni 2p is divides into three peaks, as shown in Fig. 3c. The peak at 855.1 eV is corresponded to Ni^0, while the peaks at 874.2 and 863.7 eV are corresponded to Ni^{2+} [22]. The calculated molar content of Ni^0 and Ni^{2+} are 75.7% and 24.3%, respectively. Clearly, a large amount of Ni^{2+} is reduced to Ni^0 in the process of

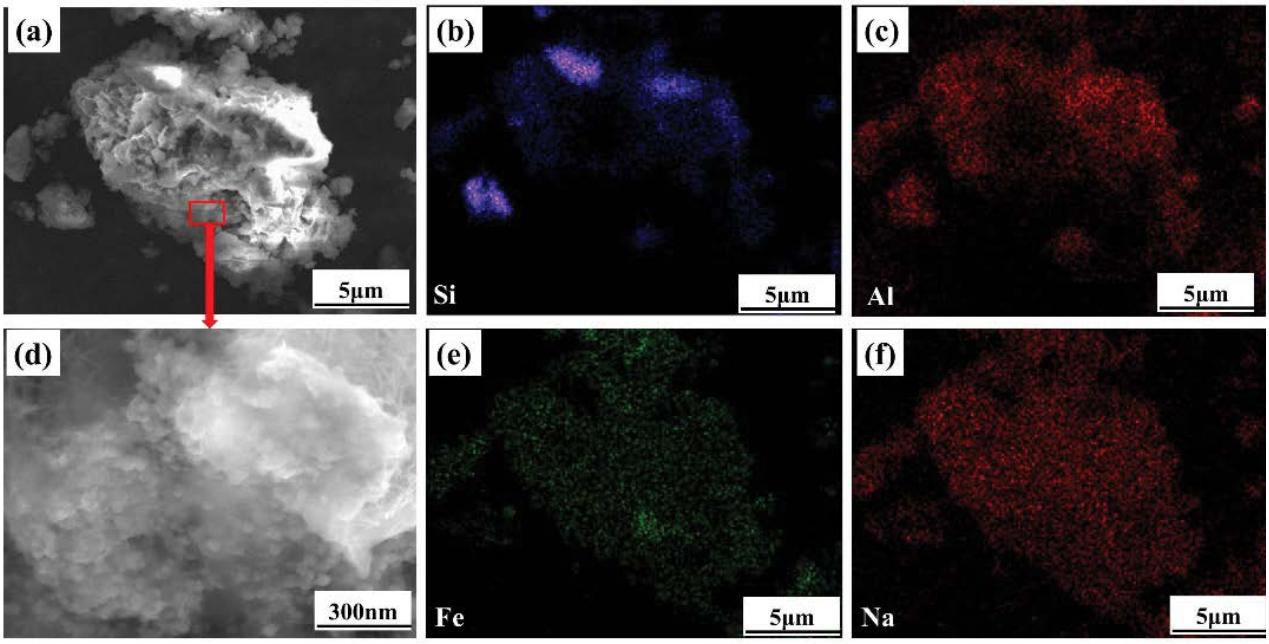

Fig. 3. SEM micrographs and mapping scan of nZVI@B, (a and d) SEM micrographs of nZVI@B, (c and d) mapping scan of nZVI@B.

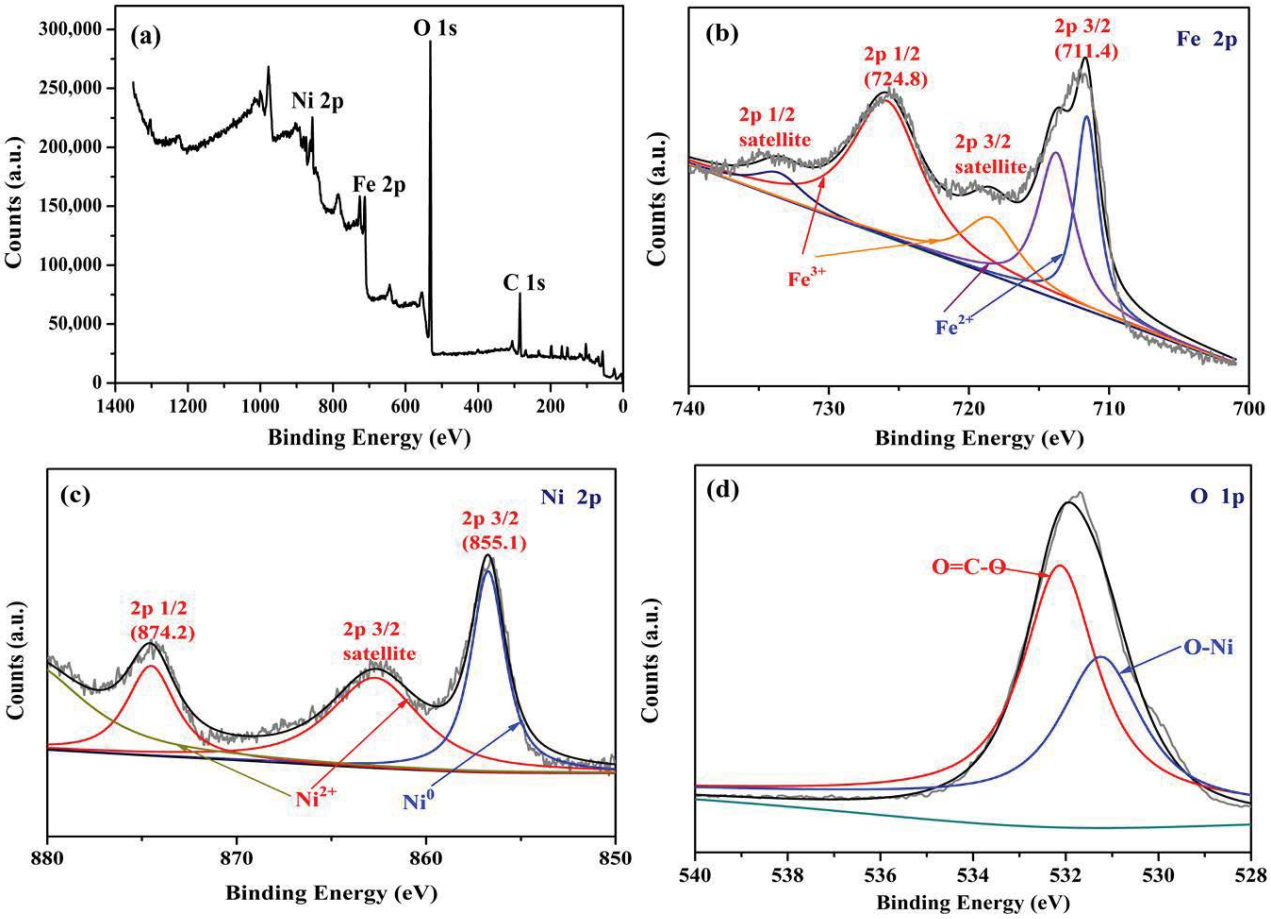

Fig. 4. XPS spectra of nZVI@B after reaction, (a) wide-scan, (b) Fe 2p, (c) Ni 2p, and (d) O1p region nZVI@B after reaction.

treatment, and it proves the reduction and adsorption is the main way for Ni^{2+} removal by nZVI@B from wastewater. Moreover, the rest of Ni^{2+} can be co-precipitation with nZVI@B. The possible reactions can be summarized as follows:

$$Fe^0 + Ni^{2+} \rightarrow Fe^{2+} + Ni^0 \quad (5)$$

$$2Fe^{2+} + Ni^{2+} \rightarrow 2Fe^{3+} + Ni^0 \quad (6)$$

$$(1-x)Fe^{3+} + xNi^{2+} + (3-x)OH^- \rightarrow Fe_{(1-x)}Ni_x(OH)_{(3-x)} \downarrow \quad (7)$$

3.2. Adsorption performance

The removal efficiencies of Ni from wastewater by bentonite, nZVI, and nZVI@B were investigated. Because of the excellent ion exchange capacity, Bentonite has a certain adsorption ability to remove Ni from wastewater, and its removal efficiency is 55.7% after 120 min, as shown in Fig. 5a. The removal efficiency of nZVI is 71.8% at 120 min. It is noteworthy that, nZVI shows a rapid removal efficiency of Ni in the initial stage of the reaction, but the removal efficiency significantly reduces with the increase of reaction time. This is due to a layer of oxide film forms on the nZVI particle surface during the treatment process, which leads to the passivation of the material [35,36]. However, the nZVI@B material exhibits the excellent removal performance with the removal efficiency of 99.6% at 120 min, and it completely meets the China's discharge standard of wastewater. As the nZVI particles are dispersed in the interlayer of bentonite, their activity can be preserved, and hence the removal ability of nZVI for Ni can be significantly improved [37].

The kinetic fitting results are shown in Figs. 5b and c, and the kinetic parameters are summarized in Table 1. Based on R^2, the PFO model can better describe the Ni removal behavior, suggesting that the removal of Ni by nZVI@B is controlled by the adsorption process [38]. Clearly, the rate constant k_1 of nZVI@B is 0.0343 min^{-1}, which is higher than that of Bentonite and nZVI, indicating that the nZVI particles supported on bentonite can be significantly improved its reactivity. In this study, the removal performance of nZVI@B has been compared with that of other nZVI combined materials reported in the literatures, as shown in Table 2. Obviously, the removal performance of nZVI@B is outstanding, and it has great potential for removing Ni^{2+} the from the actual electrolytic wastewater.

The effect of different initial pH values of wastewater ranging from 3.0 to 10.0 on Ni removal by nZVI@B was investigated, as shown in Fig. 6a. When the initial pH value

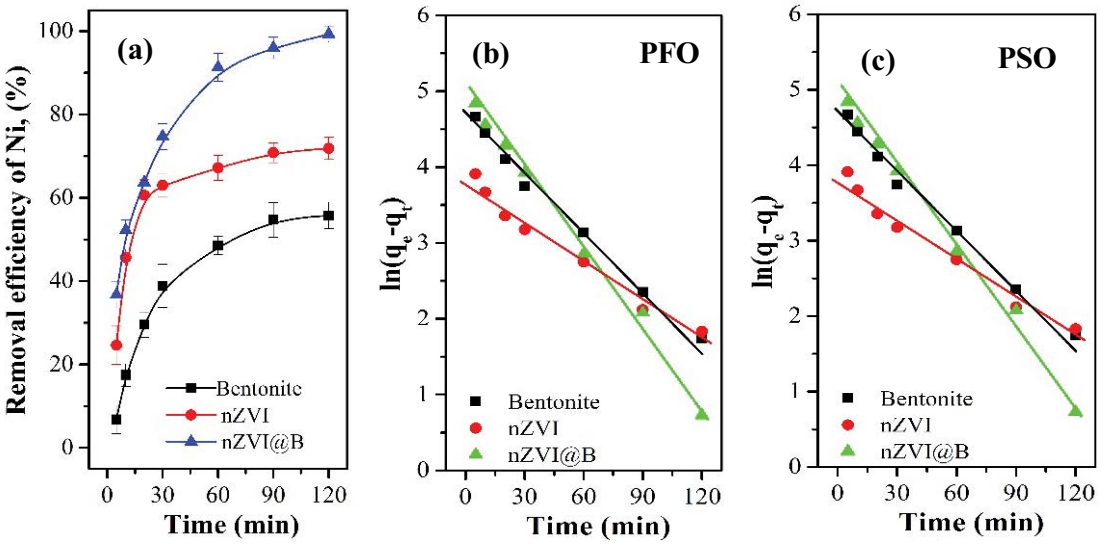

Fig. 5. (a) Removal efficiencies of Ni using different materials, the experiment conditions were the initial concentration of 10 mg/L, dosage of 20 mg/L, pH value of 4.7, and temperature of 20°C, (b) and (c) the kinetic analysis of reduction–adsorption of Ni using PFO and PSO.

Table 1
Kinetic parameters for Ni removal by bentonite, nZVI, and nZVI@B

Sample	PFO			PSO		
	q_e (mg/g)	k_1 (min^{-1})	R^2	q_e (mg/g)	k_2 (g/mg min)	R^2
Bentonite	58.73	0.0249	0.9919	57.14	0.0067	0.9713
nZVI	75.14	0.0176	0.9757	73.21	0.0021	0.7916
nZVI@B	99.76	0.0343	0.9953	102.02	0.0017	0.8129

Table 2
Comparison of Ni removal with different absorbents reported in the literatures

Absorbent	Dosage[a] (mg/L)	Initial pH	Initial concentration (mg/L)	T (°C)	Reaction time (min)	Removal capacity %	Reference
nZVI@GC	50	5	20	30	120	87.80	[40]
nZVI@AC	25	7	10	20	30	91.21	[41]
nZVI@S	50	5	10	20	180	92.31	[42]
nZVI@B	20	4.7	10	20	120	99.60	This study
nZVI	20	4.7	10	20	120	71.80	This study

GC: Mesoporous carbon; AC: activated carbon; S: *S. cerevisiae* cells; dosage[a]: only present Fe.

is 3.0, the removal efficiency is 93.4% at 120 min. The removal efficiency of Ni is high in the initial stage of the reaction and significantly reduces with the extension of time. This may be due to the rapid dissolution of the oxide layer on the surface of nZVI particles under acidic conditions, and the dissolution process improves the activity of nZVI but accelerates its consumption [31–33]. The removal efficiency reduces to 74.3% at 120 min when the pH value is 10.0. Alkaline condition promotes the formation of hydroxide passivation layer on the surface of nZVI, thereby inhibiting its activity [34,35]. It should be noted that the final pH values of solutions after 120 min reaction time are in the range of 6.5–7.5.

Fig. 6b shows the removal efficiency of Ni by nZVI@B under different initial concentrations of Ni in wastewater ranging from 10 to 100 mg/L. With the increase of initial concentration from 10 to 100 mg/L, the removal efficiency of Ni decreased from 99.96% to 98.57%. However, the removal efficiency is obviously reduced in the initial stage of the reaction. The highly initial concentration leads to a competition effect among target pollutants and activity sites on the surface of nZVI@B, which leads to the reduction

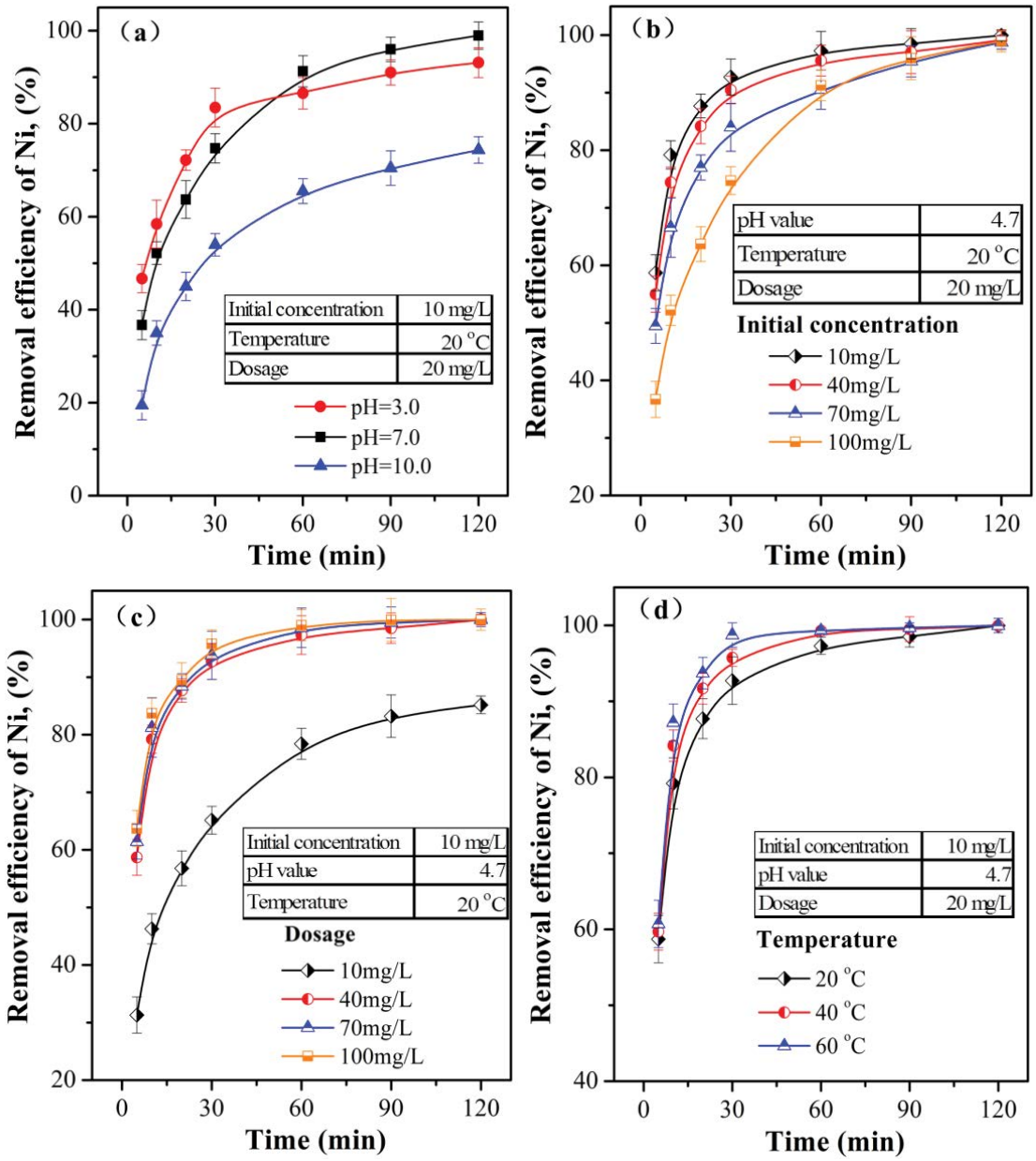

Fig. 6. Effects of experiment parameters on removal efficiency.

of Ni removal efficiency [39]. In addition, the surface of nZVI particles is easier to passivate with the increase of initial concentration, and the electron transfers between nZVI and discharge standard are inhibited, resulting in the reduced of removal efficiency.

Fig. 6c presents the effect of dosage on removal efficiency of Ni. It can be seen that the removal efficiency of Ni has an enormous increase, as the dosage increases from 10 to 40 mg/L. This is because when the dosage is not enough, the active site of nZVI is not enough, resulting in the relatively low removal efficiency. However, as the dosage continuous increases from 20 to 40 and 60 mg/L, there is no significant difference. The removal efficiency of Ni at 120 min can reach 99.5%.

Fig. 6d shows the effect of temperature on removal efficiency of Ni. The chemical reaction rate and the diffusion rate of Ni in the solution can be increased by the higher temperature during the reaction process, so as to improve the removal efficiency. However, if the dosage is enough, the effect of temperature on final removal efficiency (at 120 min) is not remarkable.

3.3. EDX analysis of tailings

The tailings obtained by batch experiments under different initial pH values were dried and detected by EDX. The results are shown in Table 3, and the sample (a), (b), and (c) are corresponded to pH values of 3.0, 7.0, and 10.0,

Table 3
EDS results of nZVI@B after reaction, wt.%

Sample	Ni	Fe	Si	Al	Na	Ca
(a)	33.766	29.771	21.0782	11.9628	2.153	1.269
(b)	38.556	22.811	27.3715	8.2055	1.877	1.179
(c)	27.672	33.248	28.6182	8.4068	1.434	0.621

respectively. The content of Ni is in the range from 25% to 40%, which reduces the total amount of tailings treatment and the difficulty of recycling. There are two reasons for the reduction of the amount of tailings. First, it comes from the excellent removal capacity of the nZVI@B. Second, due to the simpler use of the nZVI@B, the acidifying or alkalizing agent and flocculant is not need to be added. Hence, the test results of tailings further demonstrate that nZVI@B could be practically applied to heavy metal pollutant adsorption and reduction.

4. Conclusion

In summary, nZVI@B was prepared by emulsion of nZVI and sodium bentonite, and used for effective removal of Ni from wastewater. The characterizations of nZVI@B through SEM, XRD, and XPS suggested that aggregation and oxidation of nZVI particles are decreased with the successful supported on bentonite. The reactivity of the nZVI can be effectively improved by dispersed in the interlayer of bentonite and reduced to contact with water. Compared with nZVI and bentonite, the removal efficiency of nZVI@B is better, which reached 99.96% at 120 min. The PFO model can fit the Ni removal behavior very well, which indicates that the removal by nZVI@B is controlled by the adsorption process. The effect of initial pH values, initial concentrations of Ni, dosage, and temperature on Ni removal were also studied in batch experiment, and results revealed that the lower solution pH value, initial concentration, and higher dosage had positive effects on Ni removal. But the effect of temperature on final removal efficiency was not remarkable. Furthermore, the tailings obtained by batch experiments was detected by EDX, the content of Ni is in the range from 25% to 40%, which reduces the total amount of tail slag treatment and the difficulty of recycling.

Funding

This study was funded by the Natural Science Foundation of Hunan Province, China (No. 2019JJ60062). National University Student Innovation Program of China (No. 201811535020).

Acknowledgments

We appreciate the students Guoliang Li and Lang Liu from the Hunan University of Technology, for them assistance on the instrument used.

References

[1] C. Blöcher, J. Dorda, V. Mavrov, H. Chmiel, K.A. Matis, Hybrid flotation-membrane filtration process for the removal of heavy metal ions from wastewater, Water Res., 37 (2003) 4018–4026.
[2] L. Botha, J.B.P. Soares, The influence of tailings composition on flocculation, Can. J. Chem. Eng., 93 (2015) 1514–1523.
[3] S. Cheng, Heavy metal pollution in China: origin, pattern and control, Environ. Sci. Pollut. Res., 10 (2003) 192–198.
[4] S. Curteanu, C.G. Piuleac, K. Godini, G. Azaryan, Modeling of electrolysis process in wastewater treatment using different types of neural networks, Chem. Eng. J., 172 (2011) 267–276.
[5] F. Fu, Q. Wang, B. Tang, Fenton and Fenton-like reaction followed by hydroxide precipitation in the removal of Ni(II) from NiEDTA wastewater: a comparative study, Chem. Eng. J., 155 (2009) 769–774.
[6] G. Guglielmi, D. Chiarani, S.J. Judd, G. Andreottola, Flux criticality and sustainability in a hollow fibre submerged membrane bioreactor for municipal wastewater treatment, J. Membr. Sci., 289 (2007) 241–248.
[7] H. Zhang, A.M. Omer, Z. Hu, L.Y. Yang, C. Ji, X.K. Ouyang, Fabrication of magnetic bentonite/carboxymethyl chitosan/sodium alginate hydrogel beads for Cu(II) adsorption, Int. J. Biol. Macromol., 135 (2019) 490–500.
[8] P. Huang, Z. Ye, W. Xie, Q. Chen, M. Yao, Rapid magnetic removal of aqueous heavy metals and their relevant mechanisms using nanoscale zero valent iron (nZVI) particles, Water Res., 47 (2013) 4050–4058.
[9] H. Yoon, Y.G. Kang, Y.S. Chang, J.H. Kim, Effects of zerovalent iron nanoparticles on photosynthesis and biochemical adaptation of soil-grown *Arabidopsis thaliana*, Nanomaterials, 9 (2019) 1543–1555, doi: 10.3390/nano9111543.
[10] B.Q. Jiang, J.N. Zeng, Y.D. Liu, W.L. Zhang, Separation of Ni(II) from nickel-containing wastewater in an emulsion liquid membrane system with P507 as carrier, Adv. Mater. Res., 235 (2011) 837–840.
[11] L. Jing, C. Qi, X. Li, M. Yao, Rapid point-of-use water purification using nanoscale zero valent iron(nZVI) particles, Sci. Bull., 59 (2014) 3926–3934.
[12] S. Kundu, A. Aggarwal, S. Mazumdar, K.B. Dutt, Stabilization characteristics of copper mine tailings through its utilization as a partial substitute for cement in concrete: preliminary investigations, Environ. Earth Sci., 75 (2016) 221–229.
[13] T.A. Kurniawan, G.Y.S. Chan, W.H. Lo, S. Babel, Physico–chemical treatment techniques for wastewater laden with heavy metals, Chem. Eng. J., 118 (2006) 83–98.
[14] S. Li, W. Wang, F. Liang, W.X. Zhang, Heavy metal removal using nanoscale zero-valent iron (nZVI): theory and application, J. Hazard. Mater., 322 (2016) 163–171.
[15] S.K. Mehta, J.P. Gaur, Use of algae for removing heavy metal ions from wastewater: progress and prospects, Crit. Rev. Biotechnol., 25 (2008) 113–152.
[16] M. Muchuweti, J.W. Birkett, E. Chinyanga, R. Zvauya, J.N. Lester, Heavy metal content of vegetables irrigated with mixtures of wastewater and sewage sludge in Zimbabwe: implications for human health, Agric. Ecosyst. Environ., 112 (2006) 41–48.
[17] C. Peng, Y. Liu, J. Bi, H. Xu, A.S. Ahmed, Recovery of copper and water from copper-electroplating wastewater by the combination process of electrolysis and electrodialysis, J. Hazard. Mater., 189 (2011) 814–820.
[18] K. Shah, S. Ali, M. Waseem, F. Shah, A.R. Khan, Native and magnetic oxide nanoparticles (Fe_3O_4) impregnated bentonite clays as economic adsorbents for Cr(III) removal, J. Solution Chem., 48 (2019) 1640–1656.
[19] S. Zhao, H. Zhu, Z. Wang, P. Song, M. Ban, X. Song, A loose hybrid nanofiltration membrane fabricated via chelating-assisted in-situ growth of Co/Ni LDHs for dye wastewater treatment, Chem. Eng. J., 353 (2018) 460–471.
[20] T. Samaneh, J. Mohsen, Sorption and desorption of potentially toxic metals (Cd, Cu, Ni and Zn) by soil amended with bentonite, calcite and zeolite as a function of pH, J. Geochem. Explor., 181 (2017) 148–159.
[21] T. Wei, J. Fan, W. Wei, B. Nan, L. Rui, L. Yang, Y. Deng, B. Kong, J. Yang, D. Zhao, W. Zhang, Nanoscale zero-valent iron in mesoporous carbon (nZVI@C): stable nanoparticles for metal extraction and catalysis, J. Mater. Chem. A, 5 (2017) 4478–4485.

[22] P. Wu, C. Liu, Z. Huang, W. Wang, Enhanced dechlorination performance of 2,4-dichlorophenol by vermiculite supported iron nanoparticles doped with palladium, RSC Adv., 4 (2014) 25580–25587.
[23] Z. Jia, Y. Shu, R. Huang, J. Liu, L. Liu, Enhanced reactivity of nZVI embedded into supermacroporous cryogels for highly efficient Cr(VI) and total Cr removal from aqueous solution, Chemosphere, 199 (2018) 232–242.
[24] M. Gu, U. Farooq, S. Lu, X. Zhang, Z. Qiu, Q. Sui, Degradation of trichloroethylene in aqueous solution by rGO supported nZVI catalyst under several oxic environments, J. Hazard. Mater., 349 (2018) 35–44.
[25] Y. Xie, Y. Yi, Y. Qin, L. Wang, G. Liu, Y. Wu, Z. Diao, T. Zhou, M. Xu, Perchlorate degradation in aqueous solution using chitosan-stabilized zero-valent iron nanoparticles, Sep. Purif. Technol., 171 (2016) 164–173.
[26] Y. Xu, T. Dabros, J. Kan, Investigation on alternative disposal methods for froth treatment tailings-part 1, disposal without asphaltene recovery, Can. J. Chem. Eng., 91 (2013) 1349–1357.
[27] W. Yan, A.A. Herzing, C.J. Kiely, W.X. Zhang, Nanoscale zero-valent iron (nZVI): aspects of the core-shell structure and reactions with inorganic species in water, J. Contam. Hydrol., 118 (2010) 96–104.
[28] Y.Y. Zhang, H. Jiang, Y. Zhang, J.F. Xie, The dispersity-dependent interaction between montmorillonite supported nZVI and Cr(VI) in aqueous solution, Chem. Eng. J., 229 (2013) 412–419.
[29] Y.L. Yang, K.R. Reddy, Y.J. Du, R.D. Fan, Sodium hexametaphosphate (SHMP)-amended calcium bentonite for slurry trench cutoff walls: workability and microstructure characteristics, Can. Geotech. J., 55 (2018) 528–537.
[30] J. Wang, C. Zhi, D. Shao, Y. Li, S. Hu, Adsorption of U(VI) on bentonite in simulation environmental conditions, J. Mol. Liq., 242 (2017) 678–684.
[31] L.N. Shi, Y.M. Lin, X. Zhang, Z. Chen, Synthesis, characterization and kinetics of bentonite supported nZVI for the removal of Cr(VI) from aqueous solution, Chem. Eng. J., 171 (2011) 612–617.
[32] Y. Li, J. Li, Y. Zhang, Mechanism insights into enhanced Cr(VI) removal using nanoscale zerovalent iron supported on the pillared bentonite by macroscopic and spectroscopic studies, J. Hazard. Mater., 227 (2012) 211–218.
[33] B. Zhang, P. Wang, Preparation of biomass activated carbon supported nanoscale zero-valent iron (nZVI) and its application in decolorization of methyl orange from aqueous solution, Water, 11 (2019) 1671–1680.
[34] J. Xiao, Q. Yue, B. Gao, Y. Sun, J. Kong, Y. Gao, Q. Li, Y. Wang, Performance of activated carbon/nanoscale zero-valent iron for removal of trihalomethanes (THMs) at infinitesimal concentration in drinking water, Chem. Eng. J., 253 (2014) 63–72.
[35] B. Zhang, B.H. Zhu, X. Wang, S.B. You, Nanoscale zero valent iron supported by biomass-activated carbon for highly efficient total chromium removal from electroplating wastewater, Water, 12 (2020) 89–101, doi: 10.3390/w12010089.
[36] G. Sheng, X. Shao, Y. Li, J. Li, H. Dong, W. Cheng, X. Gao, Y. Huang, Enhanced removal of Uranium(VI) by nanoscale zerovalent iron supported on Na–bentonite and an investigation of mechanism, J. Phys. Chem. A, 118 (2014) 2952–2958.
[37] G. Li, Q. Xu, X. Jin, R. Li, R. Dharmarajan, Z. Chen, Enhanced adsorption and Fenton oxidation of 2,4-dichlorophenol in aqueous solution using organobentonite supported nZVI, Sep. Purif. Technol., 197 (2018) 401–406.
[38] H. Lu, J. Wang, H. Hao, T. Wang, Magnetically separable MoS_3/Fe_3O_4/nZVI nanocomposites for the treatment of wastewater containing Cr(VI) and 4-chlorophenol, Nanomaterials, 7 (2017) 303–310.
[39] H. Wang, S. Cai, L. Shan, M. Zhuang, N. Li, G. Quan, J. Yan, Adsorptive and reductive removal of chlorophenol from wastewater by biomass-derived mesoporous carbon-supported sulfide nanoscale zerovalent iron, Nanomaterials, 9 (2019) 1786–1797, doi: 10.3390/nano9121786.
[40] Z. Jia, D. Li, H. Guo, Y. Zhao, Preparation of mesoporus Fe/g-C nanocomposite and its application in nickel-containing wastewater treatment, Chem. Bioeng., 3 (2017) 19–34.
[41] U. Altuntas, D. Gungor, Nano zero-valent iron supported on activated carbon: effect of AC/nZVI ratio on removal of nickel ion from water, Global Nest J., 20 (2018) 424–431.
[42] U.A. Guler, M. Ersan, *S. cerevisiae* cells modified with nZVI: a novel magnetic biosorbent for nickel removal from aqueous solutions, Desal. Water Treat., 57 (2016) 7196–7208.